

A Silicon-Based, Fully Integrated Pulse Electron Paramagnetic Resonance System for mm-Wave Spectroscopy

Charles Chen, Payam Seifi, Aydin Babakhani

Rice University, Houston, TX, 77005, USA

Abstract — An integrated transceiver for time-domain EPR spectroscopy is implemented using a 0.13 μm SiGe BiCMOS technology. The system utilizes an on-chip resonator to study time domain relaxation behavior of paramagnetic samples, i.e. materials with unpaired electron spins. The single-chip EPR spectrometer consists of an EPR resonator, 22-26GHz tunable VCO, a programmable pulse generation block, RF buffer and power amplifier, a multi-stage LNA, and down-conversion mixer all in a 2mm²-size chip area.

Index Terms — Electron paramagnetic resonance, mm-wave, silicon, fully integrated, spectroscopy

I. INTRODUCTION

Electron Paramagnetic Resonance (EPR or Electron Spin Resonance (ESR)) is a powerful spectroscopic technique used for studying materials and processes involving unpaired electron spins. The required magnetic field in EPR is about 700 times smaller than that of NMR (for the same resonance frequency). This significantly reduces the requirements of the magnet making it possible to build a handheld EPR spectrometer. EPR is used to study properties of paramagnetic species, such as metal ions in enzymes or free radicals involved in biochemical signaling pathways. The EPR technique is capable of direct measurement of the partial pressure of oxygen ($p\text{O}_2$) in tissues with high sensitivity and accuracy [1]. EPR is also used in studying of cardiovascular diseases [2]. EPR is used for studying a special type of human skin cancer known as melanoma, where melanin pigments – naturally occurring proteins protecting against UV radiation and responsible for hair and skin color – act as ‘traps’ for free radicals that can be subsequently detected or imaged using EPR technology [3].

Currently there are two major family of techniques used to perform EPR spectroscopy. The first one is a frequency domain method using Continuous Wave (CW) EPR and the second one is a time domain technique using pulse EPR. CW utilizes a continuous, narrow-band signal to energize unpaired electrons in the presence of an external DC magnetic field (B_0), and sweeps the frequency or the DC magnetic field to obtain the absorption line shape of the sample. It has been traditionally used for EPR because it is simpler in terms of circuitry and is able to study a wide range samples, including those with broad lines or very fast relaxation times (tens of nanoseconds). However, direct measurement of certain spin relaxation parameters, such as longitudinal relaxation due to spin-lattice interaction (T_1) and transverse relaxation due to

spin-spin interaction (T_2) is feasible using time domain or pulse techniques.

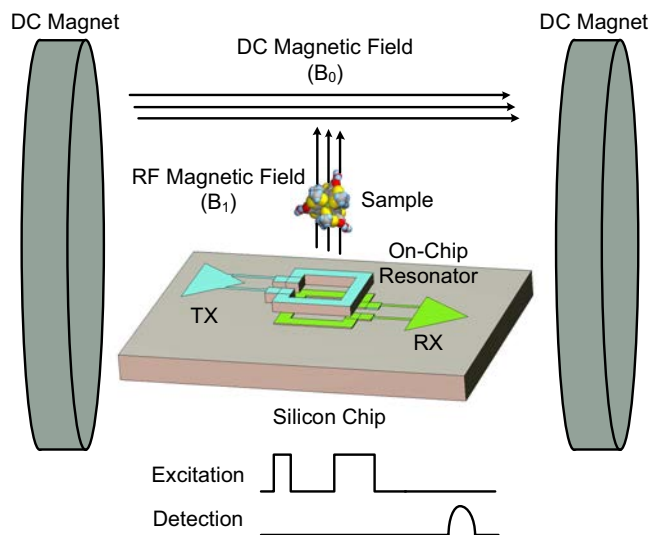


Fig. 1: Concept of pulse EPR spectroscopy. The transmitter sends two modulated RF pulses (90° and 180°) and detects the echo from the EPR sample.

In pulse EPR shown in Figure 1, instead of sweeping a continuous signal, high-energy narrow pulses are used to generate an RF magnetic field, B_1 , normal to the DC field, B_0 . The B_1 RF field flips the spins of the unpaired electrons. The subsequent time-domain signal from spin relaxation is then recorded. Wideband spectral information of the EPR samples is reproduced using Fourier transform techniques applied to the EPR transient response. EPR spectrometers traditionally consisted of discrete microwave components that are heavy, expensive and bulky. In this paper we present the first silicon-based, fully integrated mm-wave pulse EPR spectrometer capable of time-domain measurements.

II. CIRCUIT DESIGN AND IMPLEMENTATION

A block-diagram of the integrated EPR spectrometer is shown in Figure 2. During the first phase (excitation), the transmitter section provides an RF magnetic field on the EPR sample by controlling the output current of an on-chip resonator connected to a power amplifier (PA). The 30GHz B_1 magnetic field generated in the excitation coil causes flipping

of electron spins. In phase two, a control pulse signal switches off the PA in less than 0.5ns. This is implemented by switching off both the PA and its previous buffer stage, as will be explained in the following paragraphs. The sooner the transmitter turns off, the faster the time domain EPR signal can be observed. In this scheme, it is not necessary to turn off the LNA, as the LNA transition from saturation to linear operation is also about 0.5ns. In the final stage (the detection phase) the four-stage differential LNA amplifies the received EPR signal by 60dB, and sends it to the mixer for down-conversion to the baseband.

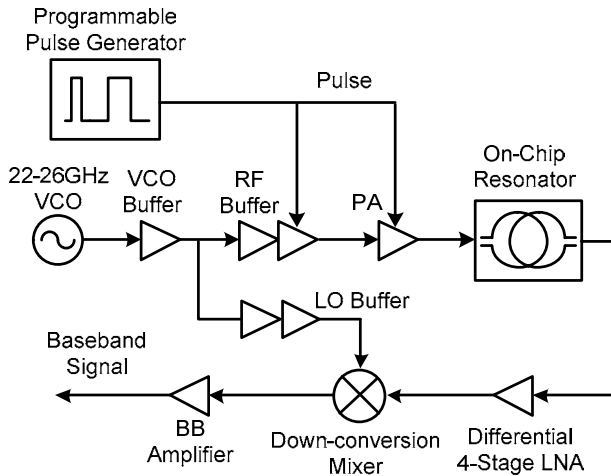


Fig. 2: The system architecture of the mm-wave EPR spectrometer.

The transmitter consists of a voltage controlled oscillator (VCO) operating at 22 GHz to 26 GHz range, buffers and a power amplifier (PA). The VCO topology used is a negative resistance cross-coupled transistor pair that provides the oscillator core. Differential transmission lines are used to bias the oscillator core as well as to serve as inductors to resonate with the varactor. The varactor is implemented using reverse-biased diodes. Following the VCO is a single-stage buffer which isolates the VCO from the PA and its preamplifier. This buffer ensures that the oscillation frequency remains unchanged by keeping the VCO load impedance constant during the transition from the excitation phase (PA on) to the detection phase (PA off). The VCO signal is then routed to the RF and LO paths, each through a two-stage buffer. In particular, the second stage of the two-stage buffer in the RF path has a switch that shorts its base voltage to ground, providing a high level of isolation between the VCO output and the on-chip resonator. The PA has a similar switching mechanism with an additional pull-down transistor at the base of the PA cascode transistor stage that provides further isolation. This operation allows for the VCO to remain on throughout all stages, eliminating start-up time issues. The combined effect of switching the buffer and the PA provides 55dB on/off ratio for the current on the excitation coil.

The spectrometer core consisting of the PA, resonator and the LNA is shown in Figure 3. The PA employs a differential cascode topology which converts the input power to an RF current on the excitation coil. In order to maximize this current, the PA output matching network is optimized using on-chip transmission lines. Top metal layers with low sheet resistances (0.007 /square for 7th layer and 0.037 /square for 5th layer) are used for the coils in order to make high quality factor resonators. The excitation coil size is 20 μm and it produces a B_1 field of 20 Gauss by a current of 16mA. This is sufficient for generating a 90 degree flip angle of ~ 100 ns long.

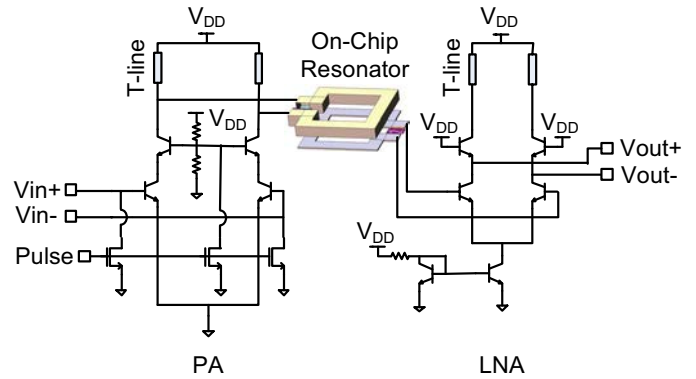


Fig. 3: Schematic of the spectrometer core consisting of the PA, on-chip loop resonators and the first stage of the 4-stage LNA (biasing not shown).

A programmable pulse generator capable of producing digital pulses with pulse widths ranging from 0.5ns-500ns is integrated, as shown in Figure 4. The pulse width is determined by the time it takes for the capacitor to discharge from the supply voltage to a threshold voltage. The “Set” signal charges the capacitor on falling edges through the pull-up PMOS transistor and discharges it through the current sources on rising edges. Ten binary scaled current sources, each representing a digital bit, control the rate at which the capacitor discharges and therefore the pulse width. This is equivalent to having pulse width resolution of 0.5ns. The comparator and the NOR gate are used to identify the rising edge of the Set signal and the rising edge of the comparator output.

On the receiver side, a four-stage variable-gain LNA providing a gain of 60dB is implemented to amplify the EPR signal. Each LNA uses differential cascode topology. The LNA input matching circuit is designed to maximize the LNA gain and match it to the detection coil. Following the LNA is a down-conversion mixer. The mixer uses double-balanced Gilbert cell topology. 50 resistors are used to degenerate the mixer in order to improve the linearity. The demodulated signal is finally amplified by the baseband amplifier which

employs a differential amplifier matched to a differential output impedance of 100 .

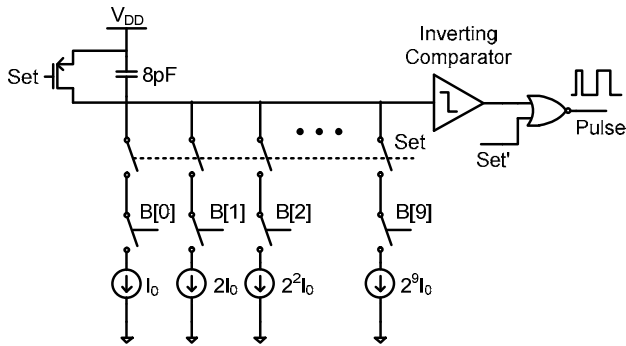


Fig. 4: Programmable pulse generation circuit. The current sources are binary scaled, allowing for programmable pulse widths with 10-bit resolution. The pulse width ranges from 0.5ns-500ns.

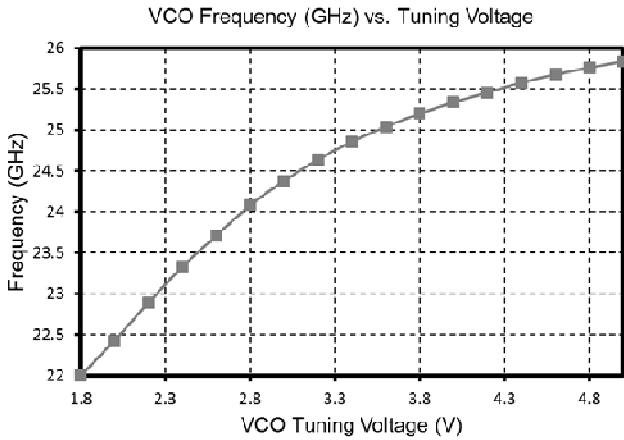


Fig. 5: Measured VCO spectrum showing the tuning range from 22-26GHz (16%).

III. MEASUREMENT RESULTS

The chip is fabricated in IBM's 0.13 μ m SiGe BiCMOS process technology. Figure 5 shows the measured VCO frequency versus the tuning voltage. The frequency ranges from 22-26GHz for a tuning voltage of 1.8V-5V, which corresponds to ~16% tuning range. The transmitter gain is 936A/W which is calculated by dividing the excitation current by the VCO output power. The receiver has a gain of 244W/A which is calculated by dividing the baseband output power on a 50 load by the detection current. The size of the chip is 1mm by 2mm. The power consumption for the whole chip is 385mW. Table 1 shows summary of the chip performance and Figure 7 shows the chip micrograph.

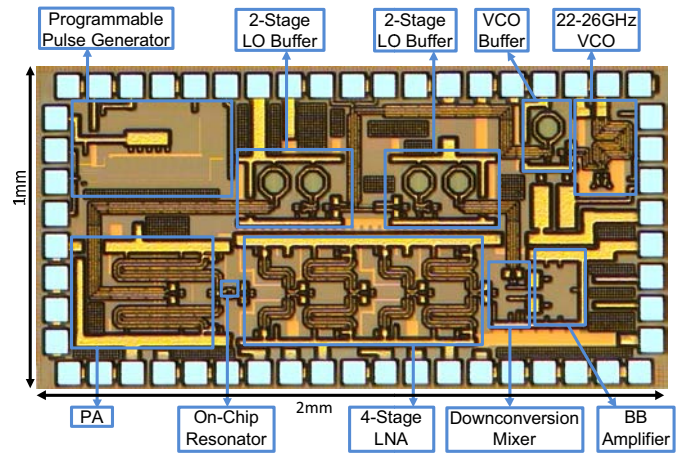


Fig. 6: Chip micrograph of the mm-wave pulse EPR spectrometer.

Table 1: Performance of the mm-wave EPR spectrometer.

SoC Specifications	
Process	IBM 8HP 0.13 μ m SiGe BiCMOS
Die specifications	1mm \times 2mm, 54 pins (47 I/O)
Power consumption	385mW
Transmitter	
Operation frequency	22-26GHz
Pulse Frequency	1-10MHz
Pulse Width	0.5ns-500ns
Pulse Resolution	0.5ns
Transmitter Gain	936A/W (excitation current/VCO output power)
Receiver	
Operation Frequency	22-26GHz
LNA Voltage Gain	61dB
Receiver Gain	244W/A (baseband output power/detection current)

REFERENCES

- [1] B. B. Williams, N. Khan, B. Zaki, A. Hartford, M. S. Ernstoff, and H. M. Swartz "Clinical Electron Paramagnetic Resonance (EPR) Oximetry Using India Ink", *Advances in Experimental Medicine and Biology*, vol. 662, pp149-156, Aug. 2010.
- [2] P. Kuppusamy and J. L. Zweier, "Cardiac applications of EPR imaging" *NMR in Biomedicine*, vol. 17, pp. 226-239, 2004.
- [3] Q. Godechal and B. Gallez, "The Contribution of Electron Paramagnetic Resonance to Melanoma Research" *Journal of Skin Cancer*, vol. 2011.